THE INTERNATIONAL JOURNAL OF MEDICAL ROBOTICS AND COMPUTER ASSISTED SURGERY
Int J Med Robotics Comput Assist Surg 2010; **6**: 221–230.
Published online 4 May 2010 in Wiley InterScience (www.interscience.wiley.com). **DOI:** 10.1002/rcs.311

ORIGINAL ARTICLE

Estimation of environmental force for the haptic interface of robotic surgery

Hyoung Il Son[1#]
Tapomayukh Bhattacharjee[2#]
Doo Yong Lee[3]*

[1]*Department of Human Perception, Cognition and Action, Max Planck Institute for Biological Cybernetics, Tübingen, Germany*

[2]*Cognitive Robotics Center, KIST, Seoul 136-791, Republic of Korea*

[3]*Department of Mechanical Engineering, KAIST, Daejeon 305-701, Republic of Korea*

*Correspondence to: Doo Yong Lee, Department of Mechanical Engineering, KAIST, 335 Gwahangno Yuseong-Gu, Daejeon 305-701, Republic of Korea.
E-mail: leedy@kaist.ac.kr

[#]These authors contributed equally to this study.

Accepted: 23 March 2010

Abstract

Background The success of a telerobotic surgery system with haptic feedback requires accurate force-tracking and position-tracking capacity of the slave robot. The two-channel force-position control architecture is widely used in teleoperation systems with haptic feedback for its better force-tracking characteristics and superior position-tracking capacity for the maximum stability margin. This control architecture, however, requires force sensors at the end-effector of the slave robot to measure the environment force. However, it is difficult to attach force sensors to slave robots, mainly due to their large size, insulation issues and also large currents often flowing through the end-effector for incision or cautery of tissues.

Methods This paper provides a method to estimate the environment force, using a function parameter matrix and a recursive least-squares method. The estimated force is used to feed back the force information to the surgeon through the control architecture without involving the force sensors.

Results The simulation and experimental results verify the efficacy of the proposed method. The force estimation error is negligible and the slave device successfully tracks the position of the master device while the stability of the teleoperation system is maintained.

Conclusions The developed method allows practical haptic feedback for telerobotic surgery systems in the two-channel force–position control scheme without the direct employment of force sensors at the end-effector of the slave robot. Copyright © 2010 John Wiley & Sons, Ltd.

Keywords force estimation; haptics; telerobotic surgery; robotic surgery

Introduction

Background

Telerobotic surgery, also known as remote surgery, provides the capacity to perform surgery on a patient at a remote location. A branch of control which deals with such telerobotic systems is called teleoperation. The concept of teleoperation enables a human operator to interact with a remote environment and perform his task with the aid of master and slave devices. A teleoperation system consists of a human operator, a local master haptic device, a communication channel, a control, a remotely located slave manipulator and the environment. In such systems, there is information exchange between the human operator and the remote environment. The information can be in the form of either position or force.

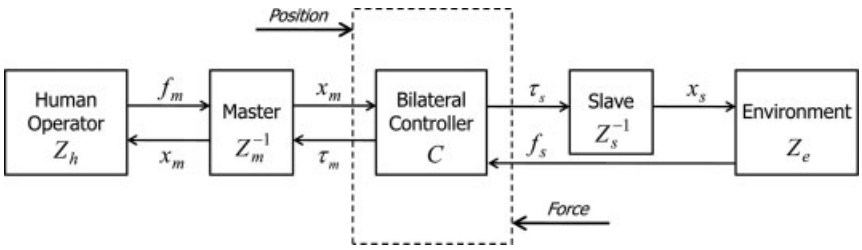

Figure 1. Simplified force–position control in a telerobotic system

Based on which information is exchanged, the control architectures are divided into four types, such as position–position control architecture (PP), force–position control architecture (FP), position–force control architecture (PF) and force–force control architecture (FF) (1). All these four control architectures are also known as 'two-channel control architectures'. If both position and force information are exchanged between the master and the slave, the control architecture is called 'four-channel control architecture' (1).

Telerobotic surgical systems in general have issues such as position tracking as well as force feedback and tracking. It is known that force–position control architecture, as shown in Figure 1, provides better force tracking control and position tracking or kinematic correspondence than position–position control architecture (1), which is essential in telesurgical procedures as it concerns the safety of the patient. The force–force control architecture has the disadvantage of position-error accumulation between the master device and the slave device (2). The position–force control architecture has practical difficulties in implementation and hence has not been used until now (2).

The force–position control architecture is shown in Figure 1; although it provides better force-tracking and position-tracking ability, it requires force information to be fed back to the surgeon, which also would provide haptic cues to the surgeon for effective surgery. Moreover, without environmental force feedback, the surgeon needs to interpret the tissue deformation and tissue behaviour to judge the force exerted by the environment, and also has to rely heavily on other accessories, which consumes time and causes mental fatigue. Many medical tasks, such as ulcer and artery localization, palpation for metastases, knot tying, quality verification of a suture, tumour detection, etc., can benefit from the environmental force which is fed back. The absence of haptic feedback can also lead to underestimated or unrecognized tissue inflammation, inability to detect solid or hollow organ masses, or accidental puncturing of blood vessels or tissue damage, and it has quite often been argued that visual information alone is highly subjective and can deteriorate because of fluids from the patient's body on the camera lens, which makes it a potential safety concern (3,4). However, force sensors, which can measure the interaction force for feeding back to the surgeon, are difficult to use in surgical cases, mainly because they are mostly positioned outside the body due to their large size, which can result in picking up unwanted friction forces and eventual distortion of force information (3,4). A force sensor, if somehow placed inside, can also lead to potential issues due to blood clotting and eventual insulation problems. One way out is, therefore, to estimate the interaction force between the slave robot and the environment so that it can be fed back to the haptic master interface to provide haptic cues to the surgeon.

Previous research

There have been many studies on environmental force estimation for non-teleoperation applications, for which the interaction force between the robot and the environment has been estimated using a disturbance observer (5,6). However, such approaches required an accurate nominal model so that the modelling error can be neglected. Also, the success of the above approaches depends on the accurate identification of other uncertainties of robotic systems, including friction. A state–space approach (7) and force observers (8) have also been used, which also required an accurate robot-dynamic model. In another study, the environment force was estimated from the difference between the disturbance observer and the disturbance observer output estimator. Friction forces and dynamic viscous effects are not considered in the modelling of robot dynamics (9).

There have been few studies to estimate the environment force in the telerobotic systems also. Katsura *et al.* (10) used disturbance observers for estimating environmental force for teleoperators, pointing out its advantage due to the large bandwidth requirement for force transmission during teleoperation. However, their method requires an accurate nominal robot model and assumes negligible modelling error. Also, the robot is assumed to operate under constant velocity, to neglect other uncertainties in the robot and the friction is assumed to have been accurately identified, which are very big assumptions (10). Another common approach involved using neural networks, but this method requires force sensors during the training phase, which is difficult in telesurgical set-ups (11). One common way of estimating environmental interaction force is based on the deflection produced on a known environmental model. However, knowing the environmental model *a priori* is also a very big assumption and is not always possible for surgical cases. An

DOI: 10.1002/rcs

environmental quarrier is proposed for bilateral telerobotic application instead of force sensors (12). Two of the same types of robot are required and they are controlled in the same position, velocity and acceleration by bilateral acceleration control, based on a disturbance observer. One robot is in contact motion and the other is unconstrained. The external force is obtained by subtracting the disturbance torque in the unconstrained robot from the constrained one. However, this method requires the use of four robots in master–slave systems. Disturbance observers have also been used for gravity estimation (13), in which gravity interferes with the manipulation of large objects. It is argued (14) that accurate sensation of force is not always desired to reproduce the force. The operator receives the reaction force not from the real environment but from the set-up environmental model. The master robot interacts with the set-up environmental model and the slave robot interacts with the real environment. However, the position error between the master and slave robots might emerge in this case. A strategy (15) for the haptic rendering of the virtual environment has been evaluated experimentally by means of a haptic simulation, in which the user manipulates a virtual slave within a contact environment via a new, parallel, redundant device. A force/velocity observer is employed for force sensing without additional hardware and is shown to be effective, despite using only joint angle measurements and a detailed model of the mechanism dynamics. In (16), the authors propose the use of a non-linear disturbance observer for estimation of contact forces during haptic interactions. They claim that this approach circumvents the traditional drawbacks of force sensing while exhibiting the advantages of closed-loop force control in haptic devices. In addition to the above performance objectives, the use of a disturbance observer has also been analysed for its stability properties to see whether it gives rise to any instability (17,18). However, it is seen that if certain design choices are made, the disturbance observer-based algorithms are exactly equivalent to passivity-based approaches and hence can thus share their stability properties.

There have also been studies on the estimation of environment models. Haddadi *et al*. (19) proposed a method for the online estimation of the Hunt-Crossley model, which can estimate the non-linear properties of the soft tissues. Yamamoto *et al*. (20) compared seven possible mathematical tissue models, using self-validation and cross-validation studies, and claimed that the Hunt–Crossley model can best describe the soft tissue characteristics. They also compared various estimation techniques and claimed that the recursive least-squares method is highly appropriate for surgical environments (21). The demerit of the above methods is that different models that can describe the characteristics of the varied soft and hard environments need to be chosen, and a common method for dealing with all kinds of environments is difficult to apply.

There has also been some work on providing the environmental force information to the surgeon by other methods. Zemiti *et al*. (22) proposed a method to measure the environmental interaction force using a force-sensor placed outside the body of the patient and claimed that it was not affected by the unwanted friction effects. However, their method was based on an assumption that the dynamic wrench is negligible and complete gravity compensation is possible. A hybrid model/learning-based dynamic equation of a robot was presented in order to draw upon the best features of both model- and learning-based techniques (23) because, with accurate knowledge of the dynamics of the robot, interaction forces can be estimated, which makes proper system identification a crucial step to success. It was shown that manual excitation can improve contact force estimation. An approach very different from all the others mentioned above was taken in (24). Instead of modelling or learning the robot's behaviour, the properties of the environment were modelled and the force was estimated by measuring the deformation of the environment with a visual system.

This paper focuses on the force-estimation algorithm that can be used in telerobotic surgical applications. The entire slave dynamics, including inertia, coupling, gravity, viscous and dynamic friction effects have been considered. No prior knowledge of the environmental model is assumed. The method does not need an initial accurate nominal model of the slave; rather, it effectively identifies it itself when the algorithm is run. A recursive least-squares algorithm is used to estimate the unknown parameters, including the uncertainties. The force feedback, required for the two-channel force–position control, is provided by the estimated force. This paper extends the original idea (25) to deal with irregular inputs by the human operator, and also includes frequency analysis of the simulation results. Experimental validation of the proposed method is also given.

Methods

The force–position control architecture, which has been applied to a telerobotic surgery system as mentioned earlier, is shown in Figure 2 (1), in which f_m, x_m, f_s and x_s are the force of the master, the position of the master, the force of the slave and the position of the slave, respectively. The master and the slave are modelled as second-order linear time-invariant (LTI) dynamic models, Z_m and Z_s, respectively, and the control input torques to the master and the slave are τ_m and τ_s, respectively. Impedance models of the human operator and the environment are represented as Z_h and Z_e, respectively. Bilateral controllers are expressed as $C_i, i = m, c, 1, 2, 5, 6$, where C_1 is the feed-forward position control to the slave, C_2 is the feed-forward force gain to the master, C_5 is the local force gain in the slave, C_6 is the local force gain in the master, C_m is the local position control in the master and C_s is the local position control in the slave. The human intended-force input is expressed as f_h^*.

DOI: 10.1002/rcs

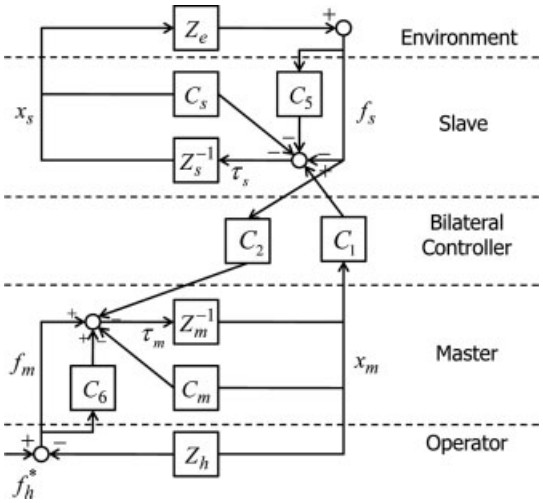

Figure 2. Generalized two-channel force–position control architecture

The input torque to the slave device is given as in equation (1) when it is not in contact with the environment:

$$\tau_s^{no\ contact} = M_s(\theta_s)\ddot{\theta}_s + C_s(\theta_s, \dot{\theta}_s) + g_s(\theta_s) + v_s\dot{\theta}_s + k_s \cdot \mathrm{sgn}(\dot{\theta}_s), \quad (1)$$

where $M_s(\theta_s)$ is the inertia matrix term; $C_s(\theta_s, \dot{\theta}_s)$ is the centrifugal and coriolis force matrix term; $g_s(\theta_s)$ is the gravity term; and θ_s, $\dot{\theta}_s$, and $\ddot{\theta}_s$ are the joint position, joint velocity and joint acceleration of the slave device, respectively (26,27).

The viscous friction term can be assumed to be in the form of $v_s\dot{\theta}_s$ and the dynamic friction term can be expressed as $k_s \cdot \mathrm{sgn}(\dot{\theta}_s)$ (27), where v_s and k_s are the coefficients of the viscous and dynamic friction, respectively, and:

$$\mathrm{sgn}(x) = \begin{Bmatrix} +1 & x > 0 \\ 0 & x = 0 \\ -1 & x < 0 \end{Bmatrix}. \quad (2)$$

A nominal model of the slave device in the telesurgical system is given by $\tilde{Z}_s = \tilde{M}_s\ddot{\theta}_s + \tilde{B}_s\dot{\theta}_s$, where $\tilde{M}_s$ and $\tilde{B}_s$ are the nominal mass and the nominal viscous or dynamic friction coefficient of the slave manipulator, respectively. Equivalent disturbance to the slave device can be in the form of equation (3):

$$\tau_s^{dis} = \left(M_s(\theta_s) - \tilde{M}_s\right)\ddot{\theta}_s + C_s(\theta_s, \dot{\theta}_s) + g_s(\theta_s) + (v_s - \tilde{B}_s)\dot{\theta}_s + k_s \cdot \mathrm{sgn}(\dot{\theta}_s) \quad (3)$$

Now, equation (3) can be rearranged to the form of equation (4):

$$\tau_s^{dis} = \mathbf{W}\boldsymbol{\Psi}, \quad (4)$$

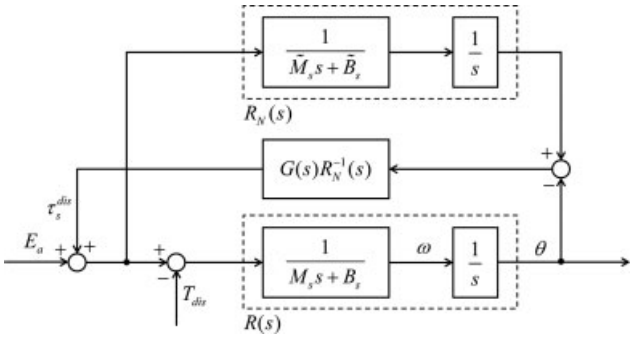

Figure 3. Model of disturbance observer

where **W** is a robot function parameter matrix dependent on joint positions, velocities and accelerations (10,27), and **Ψ** is a matrix of unknown parameters, such as masses of links (assumed as lumped point masses) and viscous and dynamic friction coefficients.

Uncertainty in the nominal model of the slave device can be reduced, and hence the behaviour would become more predictable if the disturbance torque were added to the torque input *a priori*. The model of the disturbance observer (6) is shown in Figure 3. $R(s)$ and $R_N(s)$ are the true and nominal models of the device actuator, respectively. M_s and B_s are the true mass and the true viscous or dynamic friction coefficients of the slave manipulator, respectively. T_{dis} is the actual disturbance torque to the actuator. $G(s)$ is a second-order low-pass filter with a natural frequency ω_n and given as equation (5):

$$G(s) = \frac{\omega_n^2}{s^2 + 2\omega_n s + \omega_n^2}. \quad (5)$$

The estimated disturbance torque can be computed as in equation (6):

$$\frac{\tau_s^{dis}}{T_{dis}} = \frac{\dfrac{G(s)R_N^{-1}(s)R(s)}{1 - G(s)}}{1 + \dfrac{G(s)R_N^{-1}(s)R(s)}{1 - G(s)}}. \quad (6)$$

The unknown parameter matrix can be estimated by using a recursive least-squares method. The disturbance torque can be also computed by equation (4) once the parameter matrix is updated.

A disturbance equation of the slave device can be written as equation (7) when it comes into contact with the environment:

$$\tau_s^{dis\_contact} = \left(M_s(\theta_s) - \tilde{M}_s\right)\ddot{\theta}_s + C_s(\theta_s, \dot{\theta}_s) + g_s(\theta_s) + (v_s - \tilde{B}_s)\dot{\theta}_s + k_s \cdot \mathrm{sgn}(\dot{\theta}_s) + \tau_s^e, \quad (7)$$

where $\tau_s^{dis\_contact}$ and τ_s^e are the disturbance torque of the slave device when it is in contact with the environment and the torque due to the environmental force, respectively.

DOI: 10.1002/rcs

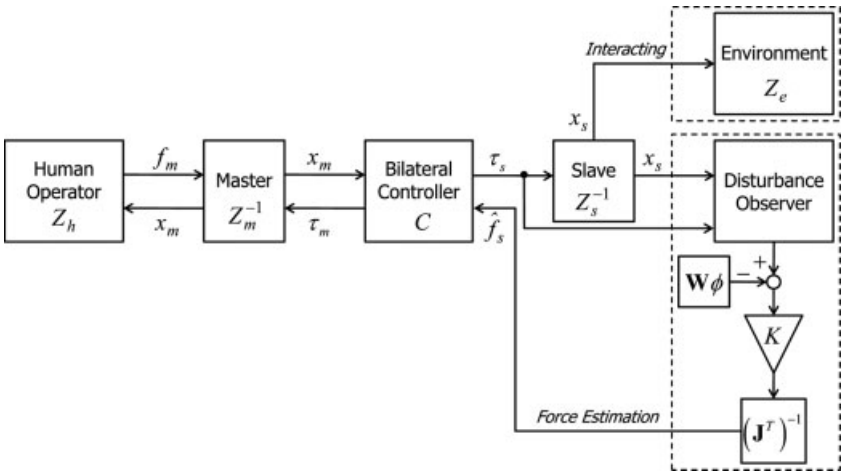

Figure 4. Simplified two-channel force–position control with the force estimation algorithm

The environmental force $\hat{f}_s$ can be found by equation (8)(10):

$$\hat{f}_s = \left(\mathbf{J}^{\mathbf{T}}\right)^{-1} K \left(\tau_s^{dis\_contact} - \mathbf{W}\boldsymbol{\Psi}\right), \tag{8}$$

where K is a gain factor and $\mathbf{J}$ is the Jacobian of the slave manipulator.

The force–position control architecture with the disturbance observer for the force estimation becomes as shown in Figure 4. The gain, K, helps to tune the magnitude of the estimated environment force, and the right choice of K depends on a specific soft tissue environment and previous experience. As a rule of thumb, we propose $K = 1$ for environments having stiffness in the order of kilo-Pascals (kPa) and $K = 10$ for stiffness in the order of mega-Pascals (MPa).

Let us now focus on the estimation of the unknown parameter matrix when the slave device is not in contact with the environment. The following recursive least-squares algorithm with the forgetting factor (28,29) is employed:

$$\boldsymbol{\Psi}_{[k]} = \boldsymbol{\Psi}_{[k-1]} + \mathbf{L}_{[k]}(\boldsymbol{\tau}_{s,[k]}^{dis} - \mathbf{W}_{[k]}\boldsymbol{\Psi}_{[k-1]}), \tag{9}$$

where:

$$\mathbf{L}_{[k]} = \frac{\mathbf{P}_{[k-1]}\mathbf{W}_{[k]}}{\lambda + \mathbf{W}_{[k]}^T\mathbf{P}_{[k-1]}\mathbf{W}_{[k]}} \tag{10}$$

$$\mathbf{P}_{[k]} = \frac{1}{\lambda}\left(\mathbf{P}_{[k-1]} - \frac{\mathbf{P}_{[k-1]}\mathbf{W}_{[k]}\mathbf{W}_k^T\mathbf{P}_{[k-1]}}{\lambda + \mathbf{W}_{[k]}^T\mathbf{P}_{[k-1]}\mathbf{W}_{[k]}}\right) \tag{11}$$

The initial guess for the adaptation gain matrix P and the forgetting factor $\lambda(0 \leq \lambda \leq 1)$ is to be determined by the user accordingly (29,30). However, we propose that $\lambda = 1$ and $\mathbf{P} = 10^5\mathbf{I}$ ($\mathbf{I}$ = Identity Matrix) are used. The change in values of the $\mathbf{P}$ matrix does not have any significant effect in the convergence of the estimation algorithm. The elements of the matrix can be stored and can be used repeatedly for subsequent operations, as this is a property of the slave manipulator, which reduces any extra computational burden and delay, as no online identification schemes are required. There is no need for any initialization period of the slave robot in subsequent operations and it would be directly available for use.

The procedure can be summarized as follows:

1. *Start operating the slave device.*
2. (Lines 2 to 17 required during first-time use only).
3. Initial guess of $\boldsymbol{\Psi}$, $\mathbf{P}$, and λ.
4. **While** (no contact with environment).
5. {
6. Disturbance output obtained.
7. $\mathbf{W}$ obtained as a function of device parameters.
8. **Repeat** 7 : 12.
9. {
10. Update $\mathbf{L}_{[k]}$.
11. Update $\boldsymbol{\Psi}$ based on RLS scheme.
12. Update $\mathbf{P}_{[k]}$.
13. }
14. Until (error of estimate > = value).
15. }
16. **End.**
17. Store $\boldsymbol{\Psi}$.
18. *Slave device makes contact with the environment.*
19. **While** (slave device is in motion).
20. {
21. Disturbance output obtained.
22. $\mathbf{W}$ obtained as a function of device parameters.
23. Recall the stored $\boldsymbol{\Psi}$ value.
24. Subtract $\mathbf{W}\boldsymbol{\Psi}$ from the disturbance output.
25. Apply gain factor K.
26. Estimate force by obtaining inverse Jacobian.
27. }
28. **End.**

Results

Simulation results

Let us now consider a one degree of freedom (DOF) telerobotic system for simulation purposes, as shown

DOI: 10.1002/rcs

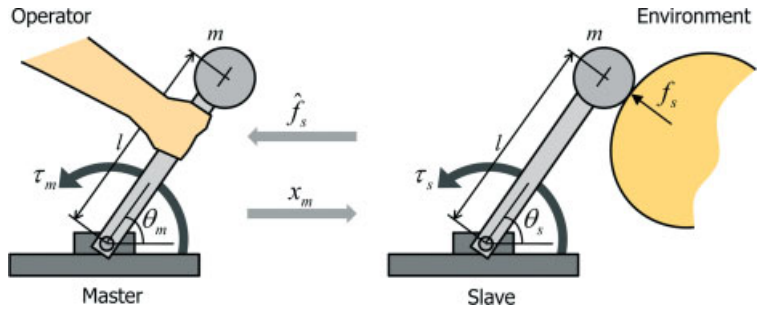

Figure 5. Simulation configuration of a one-DOF telerobotic system

in Figure 5. MATLAB Simulink was used for simulation to show the efficacy of the developed force-estimation method.

The simulated teleoperation system has a master device with a mass $\tilde{M}_m = 6$ kg, a damping coefficient $\tilde{B}_m = 0.1$ kg/s and a stiffness coefficient $K_m = 0$ N/m. Its slave device has the same mass, damping and stiffness coefficients. The master and slave manipulators are locally controlled by position compensators $C_m = 48 + 390/s$ and C_s with the same parameter values, respectively. The local force controllers for the master and the slave are assumed to have scalar gains of $C_6 = -0.5$ and $C_5 = -0.4$, respectively. It is assumed that there is no force or position scaling or time delay in the system. The master coordinating the force-feedforward controller is taken to be $C_1 = 48.1 + 390/s$, according to transparency-optimized control law (26,31). The acceleration signals are not used to avoid noise. The slave force-feedforward controller has a scalar gain of $C_2 = 0.5$. The controller values are selected such that the transparency is optimized. Impedance of the soft environment is assumed to be $Z_e = 0.5s + 0.1 + 1/s$. The operator impedance is set to $Z_h = 2s + 2 + 10/s$. The system is triggered by the exogenous input force by the operator. The torques are measured in Nm.

The equivalent disturbance torque will be as in equation (12):

$$\tau_s^{'dis} = (ml^2 - 6)\ddot{\theta}_s + mgl\cos\theta_s + (\nu_s - 0.1)\dot{\theta}_s + k_s \cdot \mathrm{sgn}(\dot{\theta}_s) \tag{12}$$

This can be expressed in a matrix notation, as in equation (13):

$$\tau_s^{dis} = \tau_{dis}^{'s} + 6\ddot{\theta}_s + 0.1\dot{\theta}_s = [\, l^2\ddot{\theta}_s + gl\cos\theta \quad \dot{\theta}_s \quad \mathrm{sgn}(\dot{\theta}_s)\,] \begin{bmatrix} m \\ \nu_s \\ k_s \end{bmatrix} \tag{13}$$

We can thus get the robot function parameter matrix and the unknown parameter matrix by comparing equations (13) and (4), and they are as equations (14) and (15), respectively:

$$\mathbf{W}^{\mathrm{T}} = [\, l^2\ddot{\theta}_s + gl\cos\theta_s \quad \dot{\theta}_s \quad \mathrm{sgn}(\dot{\theta}_s)\,] \tag{14}$$

$$\mathbf{\Psi} = \begin{bmatrix} m \\ \nu_s \\ k_s \end{bmatrix} \tag{15}$$

The simulation is first carried out when the slave is not in contact with the environment, i.e. $Z_e = 0$. The system is triggered by exogenous input force by the operator. The input torque to the slave, the slave position, velocity and acceleration are obtained. Thus, the robot function parameter matrix and the input torque are known. The link length l of the one-DOF slave manipulator is set to be 1 m and the mass as 1 kg. Using the relationship $\tau_s^{dis} = \mathbf{W\Psi}$, the unknown parameter matrix is computed using the recursive least-squares algorithm, the *lsrec* function, in MATLAB. After the unknown parameter matrix is updated, the environment impedance is changed to the original value selected for a soft environment. The estimated environment force is computed by equation (8).

Next, the simulation was performed with irregular force input from the human operator. The total simulation time was set to be 30 s with sampling time of 1 ms. The irregular human force input was simulated with a combination of various amplitudes and frequencies, as shown in Figure 6 and equation (16):

$$f_h^* = \begin{cases} \sin(\pi t) & , 0 \le t < 4 \\ 5 + 3.5\sin(\pi t) & , 4 \le t < 12 \\ 2\cos(0.5\pi t) - 0.6875t + 11.75 & , 12 \le t < 20 \\ 2\sin(2\pi t) & , 20 \le t < 26 \\ \sin(0.3333\pi t) & , 26 \le t \le 30 \end{cases} \tag{16}$$

The disturbance input to the slave robot was implemented using the white-noise function generator in MATLAB. The sampling time of the disturbance was taken to be similar to the overall sampling time of 1 kHz. The

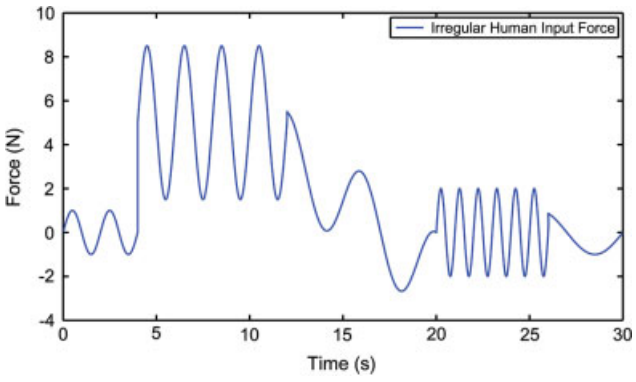

Figure 6. Irregular input force of a human operator to the master in simulation

DOI: 10.1002/rcs

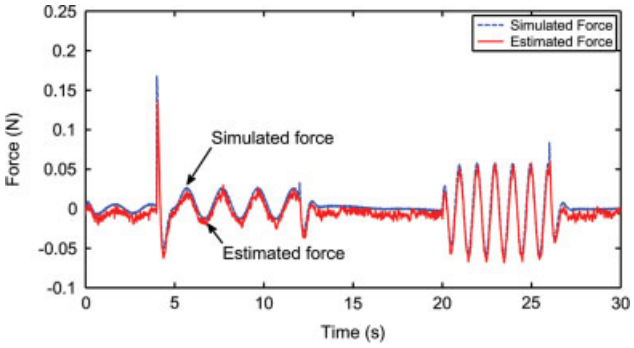

Figure 7. Simulated force and the estimated force for irregular human input motion

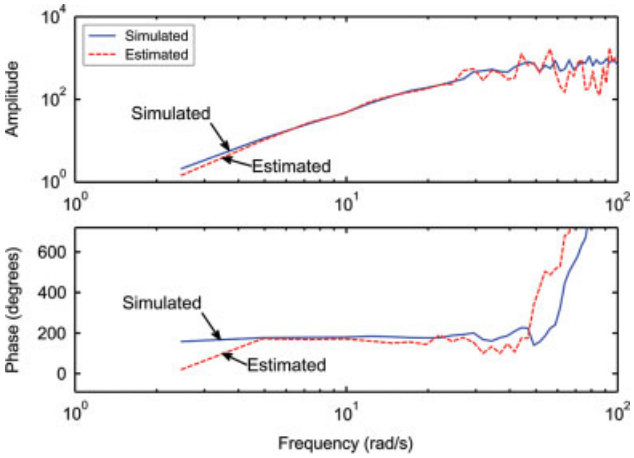

Figure 8. Bode-plot of the simulated and estimated forces for irregular human input motion

magnitude was selected by a random number generator. The frequency of the second-order low-pass filter in the disturbance observer was taken to be 20 Hz. chosen in accordance with frequency dependence for compliance contrast detection (32).

The simulation result is shown in Figure 7. The Bode plot, of the simulated force and the estimated force with the irregular force input, is shown in Figure 8. The time-domain graph shows considerable agreement between the simulated and estimated forces. The Bode-plot also shows that the simulated and the estimated forces agree well in the low-frequency region. There is some discrepancy in the estimated value in the high-frequency region of around 100 Hz. This is quite tolerable when considering the frequency range of telesurgery.

Experimental Results

The experimental set-up, as shown in Figure 9, was prepared using PHANToM as the master device and a one-DOF mechanical device as the slave manipulator. The force estimation algorithm was incorporated to compare the estimated force with the actual force obtained from a ATI FT6409 force-torque sensor attached to the end-effector of the slave manipulator. A National Instruments

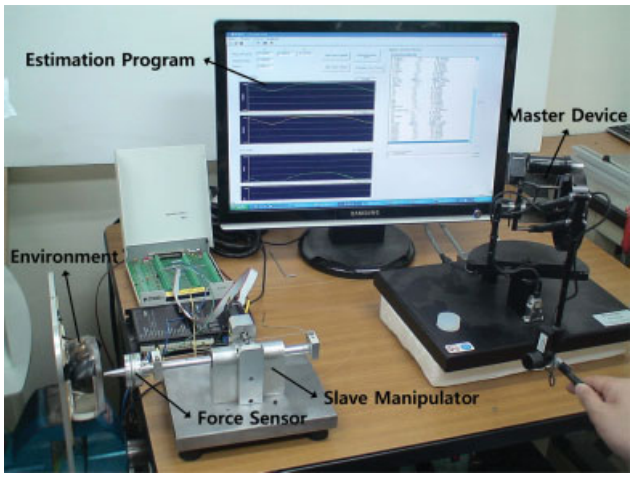

Figure 9. Experimental set-up of a teleoperation system with PHANToM as the master and a one-DOF slave interacting with phantom tissues

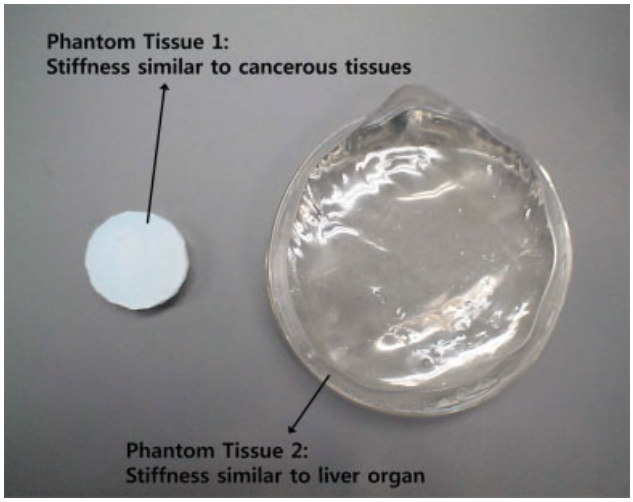

Figure 10. Samples of two types of phantom tissues

Motion Controller was used, together with a Maxon motor-driving circuit, to control the slave manipulator. The program was run using a GUI with constant interaction between C Language and MATLAB Simulink. We used two types of phantom tissues as the visco-elastic soft tissue environments, as shown in Figure 10, with a 1 : 1.5 ratio of the solvent and the hardener, to create an environment stiffness value of several MPa to approximately represent cancerous tissues (phantom tissue 1), and a 1 : 1 ratio of the solvent and the hardener to create an environment stiffness value of several kPa to approximately represent liver-like behaviour (phantom tissue 2).

The experimental results, as presented in Figures 11–14, show the efficacy of the proposed estimation algorithms. Figures 12 and 14 show that there was no increase in the tracking error due to our algorithm, and the system was stable. The magnitude of the forces was larger for phantom tissue 1, as shown in Figure 11, compared to that of Figure 13, which was expected, as

DOI: 10.1002/rcs

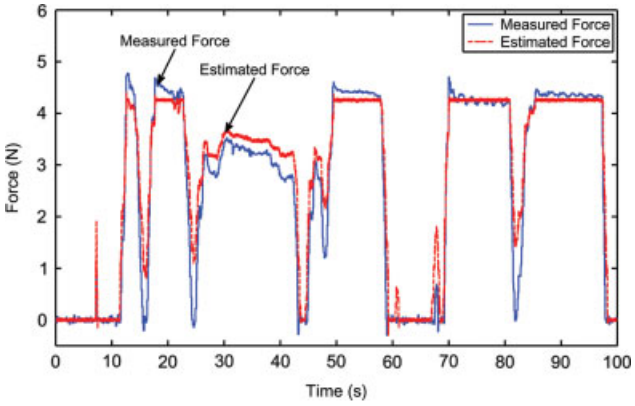

Figure 11. Measured force and estimated force for the slave manipulator interacting with phantom tissue 1

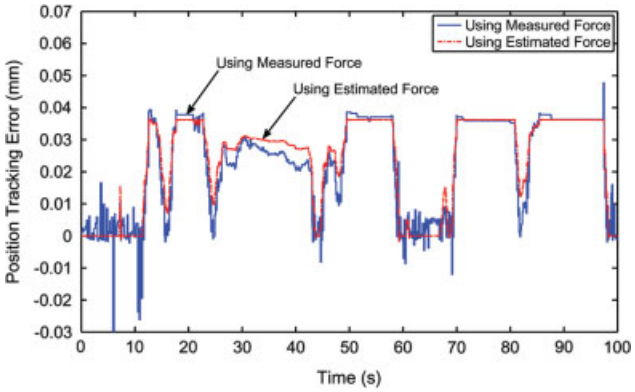

Figure 12. Comparison of master–slave position tracking errors for the slave manipulator interacting with phantom tissue 1

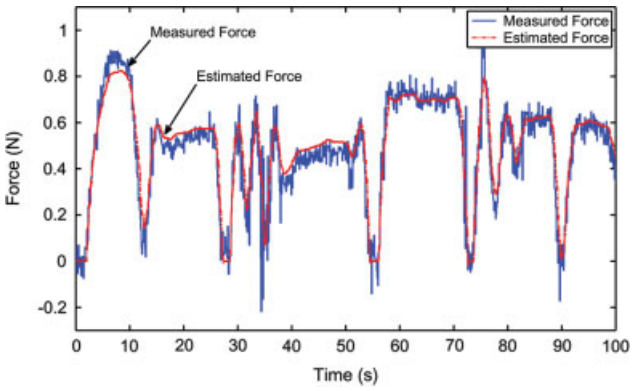

Figure 13. Measured force and estimated force for the slave manipulator interacting with phantom tissue 2

its stiffness was larger than that of phantom tissue 2. A more detailed look into Figure 11 shows that during the time periods of 12–25 and 50–60 s, the peak estimated force was slightly less than that of the measured force, but during the time period of 25–45 s the peak estimated force was slightly larger than that of the measured force. This shows that the scalar gain has to be time-varying in nature, rather than the fixed one used in this study. This presents the need for an adaptive gain selection method of the scalar gain factor K. In the time period

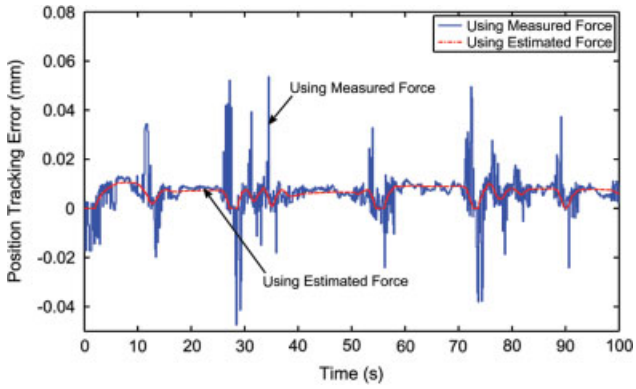

Figure 14. Comparison of master–slave position tracking errors for the slave manipulator interacting with phantom tissue 2

of 70–100 s there was very little difference between the estimated and actual forces, because the indentation of the slave manipulator into the soft tissue environment had reached its maximum limit. A detailed comparison between Figures 11 and 12 with Figures 13 and 14 shows that there are minute disturbances present in Figures 13 and 14 which show the results using phantom tissue 2. The effect of the disturbance is more for phantom tissue 2 because it is softer than phantom tissue 1, and hence the magnitude of force exerted by the environment is far less in this case. This smaller force is not negligible compared to the disturbances present in the slave robot, and hence the disturbance is reflected in Figures 13 and 14. These disturbances are, however, negligible as compared to the scale of forces exerted by the environment made of phantom tissue 1, and hence are not reflected in Figures 11 and 12.

Discussion

This paper presents a method to estimate the environmental force for the two-channel force–position haptic control architecture. This method can be used to provide force information without the direct employment of force sensors while preserving the better position tracking ability of the force–position control architecture. The developed method employs the robot function parameter matrix and the recursive least-squares method. Simulation and experimental results show that the estimation method is effective, and the error becomes negligible after a short period. The transparency is maintained without giving rise to any instability.

One interesting thing to be noticed in the experimental results, as shown in Figure 13, is that the measured force has more oscillations than that of the estimated force, and there is a little difference between the measured force and the estimated force in the high-frequency movements. This behaviour can be explained because the measured force uses a force-sensor whose resolution is higher than that of the encoder signals used to estimate the force. The measured force is thus more sensitive to minute disturbances, which are not negligible for the

environment made of phantom tissue 2. A careful look into Figure 14 shows the presence of sudden impulsive position-tracking errors, which can be explained by the same reason, the difference between the force sensor resolution or sensitivity and the encoder resolution or sensitivity. This difference in sensitivity becomes more prominent as the magnitude of the forces exerted is comparable to the disturbance produced. This explanation is further bolstered by the absence of such trends in Figure 12, wherein the slave interacts with a harder environment made of phantom tissue 1, and hence the magnitude of the disturbance is negligible.

Our force-estimation algorithm results have been shown to be accurate for a one-DOF slave manipulator. It is to be noted that we have not neglected any unwanted dynamics or disturbances and that all possible dynamic interactions have been considered. The basic motivation behind choosing a six-DOF system as a test-bed was to verify whether an algorithm works in the presence of disturbances such as coupling effects, friction and modelling errors. Since all these dynamic effects have been included in the formulation given in the manuscript, theoretically these results should extend to six-DOF systems.

However, we understand the need to demonstrate it in experiments and hence we are currently working on a six-DOF teleoperation system. We also understand that there is a considerable amount of work left to be done; however, these issues still remain as hot topics and open problems in current teleoperation research. In the future we shall also work on six-DOF force and torque estimations for complex surfaces, and this also is currently an open issue in the research community. Online time-varying tuning of the scalar gain and the application of this algorithm in cases of coupled environmental and operator dynamics also remain the subjects of future research.

Acknowledgements

This work was supported by a Korea Research Foundation grant, funded by the Korean Government (MOEHRD; Basic Research Promotion Fund) (Grant No. KRF-2008-314-D00015) and the Brain Korea 21 Project in 2008-2010.

References

1. Hashtrudi-Zaad K, Salcudean SE. Analysis of control architectures for teleoperation systems with impedance/admittance master and slave manipulators. *Int J Robotics Res* 2001; **20**(6): 419–445.
2. Gersem GD. Kinaesthetic Feedback and Enhanced Sensitivity in Robotic Endoscopic Telesurgery. PhD Dissertation, Katholieke Universitiet Leuven, Belgium, 2005.
3. MacFarlane M, Rose J, Hannaford B, *et al*. Force-feedback grasper helps restore sense of touch in minimally invasive surgery. *J. Gastrointest. Surg* 1999; **3**(3): 278–285.
4. Tavakoli M, Aziminejad A, Patel RV, *et al*. Methods and mechanisms for contact feedback in a robot-assisted minimally invasive environment. *Surg Endosc* 2006; **20**(10): 1570–1579.
5. Ohnishi K, Matsui N, Hori Y. Estimation, identification, and sensorless control in motion control system. *Proc IEEE* 1994; **82**(8): 1253–1265.
6. Ohnishi K, Shibata M, Murakami T. Motion control for advanced mechatronics. *IEEE/ASME Trans Mechatron* 1996; **1**(1): 56–67.
7. Tungpataratanawong S, Ohishi K, Miyazaki T. Force sensor-less workspace impedance control considering resonant vibration of industrial robot. In Proceedings of the IEEE Conference of the Industrial Electronics Society, 2005; 1878–1883.
8. Hacksel PJ, Salcudean SE. Estimation of environment force and rigid-body velocities using observer. In Proceedings of the IEEE International Conference on Robotics and Automation, 1994; 931–936.
9. Eom KS, Suh IH, Chung WK, *et al*. Disturbance observer based force control of robot manipulator without force sensor. In Proceedings of the IEEE International Conference on Robotics and Automation, 1998; 3012–3017.
10. Katsura S, Iida W, Ohnishi K. Medical mechatronics – an application to haptic forceps. *IFAC Annu Rev Control* 2005; **29**(2): 237–245.
11. Mobasser F, Hashtrudi-Zaad K. A model-independent force observer for teleoperation systems. In Proceedings of the IEEE International Conference on Mechatronics and Automation, 2005; 964–969.
12. Katsura S, Ohnishi K, Ohnishi K. Transmission of force sensation by environment quarrier based on multilateral control. *IEEE Trans Indust Electron* 2007; **54**(2): 898–906.
13. Nishimura K, Ohnishi K. Gravity estimation and compensation of grasped object for bilateral teleoperation. In Proceedings of the International Workshop on Advanced Motion Control, 2007; 72–77.
14. Kobayashi H, Ohnishi K. Realization of virtual force sensation through bilateral teleoperation. In Proceedings of the International Workshop on Advanced Motion Control, 2007; 323–328.
15. Sirouspour MR, DiMaio SP, Salcudean SE, *et al*. Haptic interface control – design issues and experiments with a planar device. In Proceedings of the IEEE International Conference on Robotics and Automation, 2000; 789–794.
16. Gupta A, Patoglu V, O'Malley MK. Disturbance observer based closed loop force control for haptic feedback. In Proceedings of the ASME International Mechanical Engineering Congress and Exposition, 2007; 1343–1349.
17. Bickel R, Tomizuka M. Passivity based versus disturbance observer based robot control: equivalence and stability. *J Dynam Syst Measurem Control* 1999; **121**(1): 41–47.
18. Schrijver E, Dijk JV. Disturbance observers for rigid mechanical systems: equivalence, stability, and design. *J Dynam Syst Measurem Control* 2002; **124**(4): 539–548.
19. Haddadi A, Hashtrudi-Zaad K. A new method for online parameter estimation of Hunt–Crossley environment dynamic model. In Proceedings of the IEEE/RSJ International Conference on Intelligent Robots and Systems, 2008; 981–986.
20. Yamamoto T, Vagvolgyi B, Balaji K, *et al*. Tissue property estimation and graphical display for teleoperated robot-assisted surgery. In Proceedings of the IEEE International Conference on Robotics and Automation, 2009; 4239–4245.
21. Yamamoto T, Bernhardt M, Peer A, *et al*. Techniques for environment parameter estimation during teleoperation. In Proceedings of the IEEE/RAS-EMBS International Conference on Biomedical Robotics and Biomechatronics, 2008; 217–223.
22. Zemiti N, Ortmaier T, Vitrani MA, *et al*. A force controlled laparoscopic surgical robot without distal force sensing. *Springer Tracts Adv Robotics* 2006; **21**: 153–164.
23. Naerum E, Cornella J, Elle OJ. Contact force estimation for back drivable robotic manipulators with coupled friction. In Proceedings of the IEEE International Conference on Intelligent Robots and Systems, 2008; 3021–3027.
24. Kennedy CW, Hu T, Desai JP. Combining haptic and visual servoing for cardiothoracic surgery. In Proceedings of the IEEE International Conference on Robotics and Automation, 2002; 2106–2111.
25. Bhattacharjee T, Son HI, Lee DY. Haptic control with environment force estimation for telesurgery. In Proceedings of the International Conference of the IEEE Engineering in Medicine and Biology Society, 2008; 3241–3244.
26. Craig JJ. *Introduction to Robotics – Mechanics and Control*, 2nd edn. Addison-Wesley: Reading, MA, 1986.
27. Lewis FL, Abdallah CT, Dawson DM. *Control of Robot Manipulators*. Macmillan: New York, 1993.
28. Ljung L, Sodertstrom T. *Theory and Practice of Recursive Identification*. MIT Press: Cambridge, MA, 1983.

29. Love LJ, Book WJ. Environment estimation for enhanced impedance control. In Proceedings of the IEEE International Conference on Robotics and Automation, 1995; 1854–1859.
30. Erickson D, Weber M, Sharf I. Contact stiffness and damping estimation for robotic systems. *Int J Robotics Res* 2003; **22**(1): 41–57.
31. Lawrence DA. Stability and transparency in bilateral teleoperation. *IEEE Trans Robotics* 1993; **9**(5): 624–637.
32. Dhruv N, Tendick F. Frequency dependence of compliance contrast detection. In Proceedings of the ASME Dynamic Systems and Control Division, 2000; 1087–1093.

DOI: 10.1002/rcs